Journal of Materials Science Research; Vol. 8, No. 1; 2019
ISSN 1927-0585 E-ISSN 1927-0593
Published by Canadian Center of Science and Education

Hydrogenated Nano-Crystalline Silicon Thin Films in SiO_2 Matrix for Next Generation Solar Cells Using Glow Discharged Decomposition

Moniruzzaman Syed[1], Cameron Hynes[1], Brittany Anderson[1], Temer S Ahmadi[2], Boon Tong Goh[3], Nur Fatin Farhanah Binti Nazarudin[3], Muhtadyuzzaman Syed[4] & Atif Mossad Ali[5]

[1] Division of Natural and Mathematical Sciences, Lemoyne Owen College, Memphis, TN, USA

[2] Department of Chemistry, Villanova University, Villanova, PA, USA

[3] Low Dimensional Materials Research Centre, Department of Physics, Faculty of Science, University of Malaya, Kuala Lumpur, Malaysia

[4] Department of Electrical and Computer Engineering, Purdue University, West Lafayette, IN, USA

[5] Department of Physics, Faculty of Science, King Khalid University, Abha, KSA

Correspondence: Moniruzzaman Syed, Division of Natural and Mathematical Sciences, LeMoyne-Owen College, Memphis, TN, USA. Tel: 1-267-241-2713 E-mail: moniruzzaman_syed@loc.edu

Received: November 1, 2018 Accepted: November 30, 2018 Online Published: December 31, 2018

doi: 10.5539/jmsr.v8n1p25 URL: https://doi.org/10.5539/jmsr.v8n1p25

Abstract

Hydrogenated Nanocrystalline Silicon (nc-Si:H) thin films using SiH_4/H_2 mixture by glow discharged decomposition were investigated on c-Si and glass substrates. The effects of substrate temperature on the Structural, Optical and Electrical properties of the films were investigated by X-ray diffraction, Raman scattering, FT/IR, Optical transmission and Atomic Force Microscopy (AFM). Substrate temperatures ([T_{SB}]) of the films were changed from 100°C to 250°C. It has been revealed the strong dependence on the film's properties with the substrate temperatures. XRD and Raman measurements were shown that the higher substrate temperature (250°C) exhibits the highest crystalline volume fraction ([ρ] = 95%) and the lowest crystalline size ([Ω] = 3.5 nm) as well, having the highest H-content and the lowest O-content. At 250°C, the lowest mobility and the highest resistivity were also found to be ~37.5 cm^2/v.s and 7.35 Ω-cm. Refractive index and the optical energy gap (E_g) were estimated by 3.8 and 1.9 eV having the growth rate of 4.2 nm/min. At 250°C, it was resulted in a blue shift of the absorption edge having uniform grain distributions. Results indicate that *in situ* hydrogen cleaning effects is prominent and localized orderly high density Si-Si bonds are exhibiting quantum size effects at highest substrate temperature.

Keywords: Nano-Silicon, Thin Films, Glow discharge decomposition and AFM

1. Introduction

Hydrogenated nanocrystalline silicon (nc-Si:H) thin films has attracted as a promising material in the application of optoelectronic devices such as solar cells, thin film transistors due to the quantum size effects of silicon nanocrystallites implanted in amorphous silicon medium (Gudovskikh et al., 2004). The photoluminescent intensities and band gap of these nano-materials are found to be increased with the existence of Si nano-crystallites. Luminescent properties of these films are found to be strongly reliant on crystallite size and crystalline volume fraction of nano-crystallites Si in the films (Liu et al., 1995). Various techniques have been used to prepare nc-Si:H films, including plasma enhanced chemical vapor deposition (PECVD)], electron beam evaporation, electron cyclotron resonance plasma CVD, magnetron sputtering, hot-wire CVD and Si ion implantation. Among these deposition techniques, only PECVD had been established for industrial applications. However, the crystallite size and crystalline volume fraction are not controllable by the preparation conditions. In order to enhance the device performance, improving the crystal quality using lower temperature is one of the pressing outlines in the use of PECVD.

The present work deals on exploring the influence of the substrate temperature on the growth rate, optical, electrical and structural properties of nc-Si:H films grown by conventional glow discharge system.

2. Method

The nc-Si:H thin films of ~200 nm were prepared by a home-built 13.56 MHz plasma enhanced chemical vapor deposition (PECVD) system (Figure 1) using SiH_4/H_2 mixture in a fused quartz reactor employing capacitively coupled by two parallel electrodes with a distance of 5 cm and area of 28 cm^2 and inserted into an electric furnace (Ritikos et al., 2009). The samples were deposited on corning 7059 glass substrates for X-ray diffraction (XRD), Raman scattering measurements, and on p-type boron doped (111) single crystal silicon (c-Si) wafer of a high resistivity for infrared (IR) absorption measurements. The plasma pretreatment for these substrates was performed via the same method using the above-mentioned PECVD instrument. The sample preparation process can be divided into three steps. (1) The substrates were cleaned for 15 min using acetone and for 15 min using ethanol in an ultrasonic cleaner. (2) The cleaned substrates were treated by exposing them for 20 min to H_2 plasma excited using RF power value of 80 W. (3) Finally, nc-Si:H films were prepared at 5 different substrate temperatures of 100 °C, 150 °C, 200 °C and 250°C. The conditions of the plasma pretreatment for the substrates and the film deposition conditions are summarized in Table I.

The structural properties were investigated using an XRD instrument (SIEMENS D5000 X-ray diffractometer, λ = 1.54 Å). The XRD spectra were recorded in the 2θ range from 20° to 80° at a fixed grazing angel of 5° and a scan rate of 0.02°/s. In the present study, any difference in the film thickness was corrected using the X-ray absorption coefficient for Si. Thus, the XRD intensities observed for different films can be compared. The average crystallite size, **[δ],** was estimated from the width of the XRD spectra using Scherrer's formula (Cullity, 1978).

The Raman spectra of the films were recorded using a portable iRaman (B&W TeK) with the argon ion laser having an excitation wavelength of 514 nm was used and the power was less than 5 mW. The crystallinity (crystalline volume fraction), [ρ], was estimated from the intensity ratio of the Raman spectra of a-Si phase (~480 cm^{-1}) to those of c-Si phase (~520 cm^{-1}) using the method suggested by Tsu et al. (1982).

The surface morphologies of nc-Si:H films were examined by AFM (Agilent 5500 non-contact mode). The topological images were taken by scanning electron microscopy (SEM, 1450VP, Phenom Pure).

The IR absorption was measured by a Perkin-Elmer System 2000 FTIR spectroscopy with the wavenumber range of 400 to 4,000 cm^{-1} and resolution of 2 cm^{-1}. The hydrogen content, C_H and the microstructure parameter, R of the film were determined from the Si-H wagging and Si-H/Si-H_2 stretching bands at around 630 cm^{-1} and 2000 cm^{-1} respectively using Roszairi and Rahman (2002).

The optical reflectance spectra of the films were obtained using a JASCO V570 ultra-violet visible near-infrared (UV–VISNIR) spectrophotometer. The scanning range was fixed at 2,200–220 nm with the interval of 2 nm. The reflection angle of the measurement was fixed at 5 from the horizontal plane.

Electrical resistivity of nc-Si:H thin films was determined by the dc four-probe resistivity technique in the temperature range 15-300 K on glass substrate.

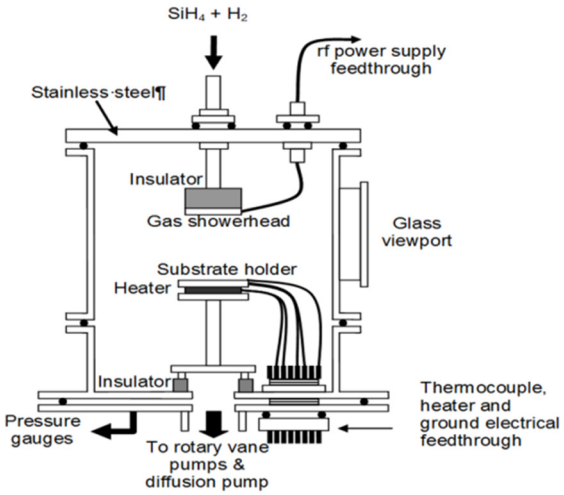

Figure 1. Schematic diagram of the glow discharged decomposition reactor

Table I. Conditions for plasma pretreatment of substrates and deposition of nc-Si:H Thin films

Plasma Pretreatment	Deposition Parameters	
$[P_{PI}]$ = 0.8 mbar	$[P_{DEP}]$ = 0.8 mbar $[H_2]$ = 100 sccm	Substrate: Glass
$[RF_P]$ = 80 W	$[t_D]$ = 1 hour P-type c-Si for IR	
$[H_2]$ = 100 sccm	$[SiH_4]$ = 2 sccm $[RF_D]$ = 80W	
$[t_P]$ = 10 min	$[T_{SB}]$ = 100ºC, 150ºC, 200ºC and 250ºC	
Corning 7059	PECVD (13.56 MHz) system	

3. Results

3.1 Evaluation of Growth Rate and Refractive Index measurements

Figure 2 shows the deposition rate ($[R_D]$) and refractive index ([n]) of nc-Si:H as a function of substrate temperature $[T_{SB}]$. In the glow discharged decomposition process both SiH4 and H_2 gas are contributed to the growth rate by dissociating and subsequent secondary reactions with reactive species of the gas molecules. Plasma pretreatment of substrates has been done with H etching with the dissociation of H_2 molecules (Matsuda, 2004). As shown in this diagram, both deposition rate and the refractive index are increasing with increasing substrate temperature from 100ºC to 200ºC with almost similar slope. However at higher temperature (250ºC) $[R_D]$ and [n] are increasing with high slope. With careful observation it is recognized that there are two distinct natures of variation of $[R_D]$ and [n] signifying a radically different growth process in effect.

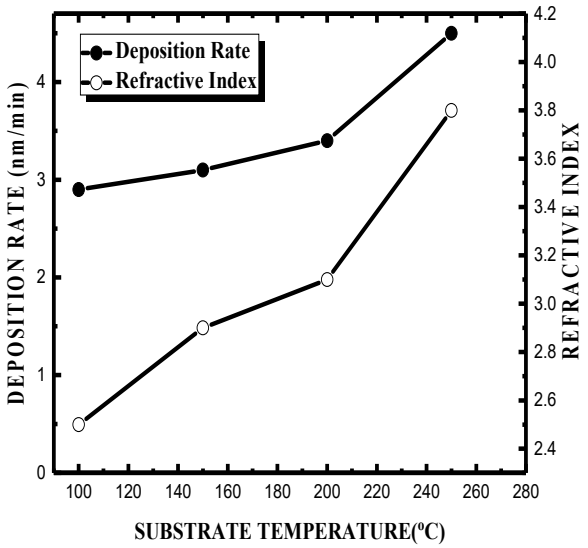

Figure 2. Deposition rate, $[R_D]$ and refractive index, [n] dependence of nc-Si:H thin films as a function of $[T_{SB}]$

3.2 Structural Properties using Raman Spectroscopy

Raman spectroscopy is a very powerful non-destructive method used to investigate the structure of materials because it gives a fast and simple way to determine the phase of the material, whether it is amorphous, crystalline or nanocrystalline.

Figure 3 shows the Raman spectra of nc-Si:H films as a function of $[T_{SB}]$ from 100 to 250^{O}C. As shown in this diagram, a strong Raman peak (I_C) at around 580 cm^{-1} for crystalline silicon (c-Si) and peak (I_a) for amorphous silicon (a-Si) at around 480 cm^{-1} are observed for all the films deposited on glass substrates. The intensity of Raman peak at around 580 cm^{-1} is found to be increased with increasing $[T_{SB}]$ having maximum at 250 ºC.

Crystalline volume fraction [ρ] has been estimated from the deconvolution of the spectra at around 480cm^{-1} and 580 cm^{-1} respectively using the following equation:

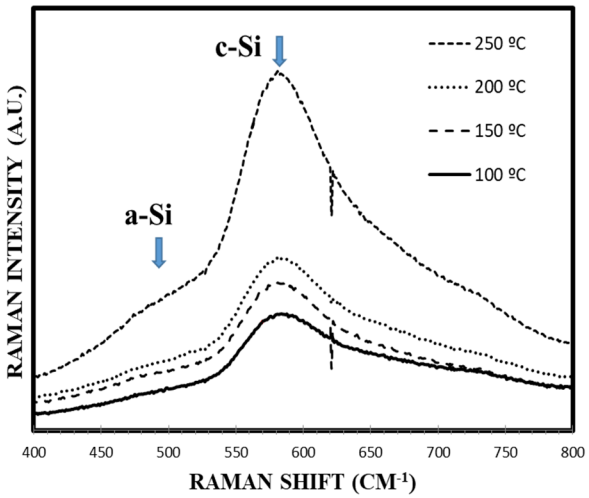

Figure 3. Raman spectra for nc-Si:H thin films deposited on glass substrates at different substrate temperature ([T_{SB}])

$$[\rho] = \frac{I_{580}}{\alpha(I_{580+I_{480}})} \quad (1)$$

where I_{580} and I_{480} are integrated intensities of the Raman peaks corresponding to crystalline and amorphous phases respectively. The factor α is generally equal to 1 for nc-Si films. The crystallite size of the Si nanocrystallites in the films can be estimated using the following equation:

$$[\Omega] = 2\pi\sqrt{\frac{B}{\Delta\omega}} \quad (2)$$

where B is 2.24$cm^{-1}nm^2$ for Si and Δω is the peak shift compared to c-Si peak located ~580 cm^{-1}.

As shown in Figure 4 Crystalline volume fraction [ρ] increases systematically from 40 % to 95 % as [T_{SB}] increases from 100ºC to 250ºC. On the other hand, crystallite size, [Ω] decreases with increasing [T_{SB}]. The smallest crystalline size has been found ~2.5 nm at ρ = 95%.

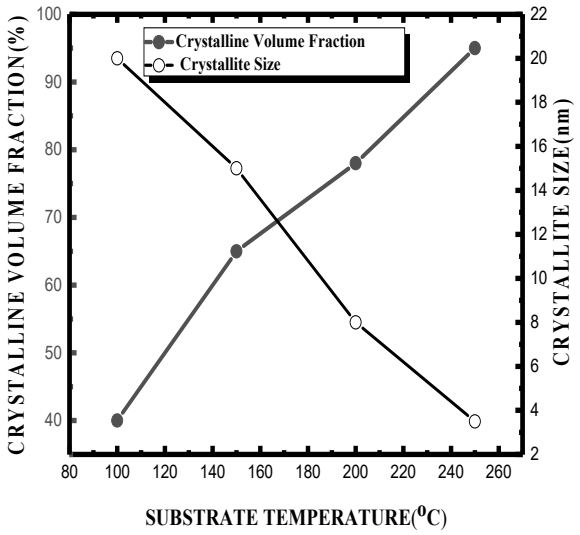

Figure 4. Crystallinity (crystalline volume fraction), [ρ] and crystallite size, [Ω] for the nc-Si:H films deposited on glass substrates (pretreatment with H_2-plasma before deposition) as a function of [T_{SB}]. These measurements were performed within one day after deposition. The solid lines are drawn as a visual reference

3.3 Structural Properties Based on XRD Measurements

Figure 5 shows the XRD spectra of nc-Si:H films deposited on glass substrates as a function of [T_{SB}]. All nc-Si:H thin films except for the films deposited at 100ºC and 150ºC show diffraction peaks at 2θ angle of 28.4º and 47.3º corresponding to c-Si orientation of <111> and <220> planes respectively showing that these films contain nc-Si phase (Ray, Mukhopadhyay, Jana, & Carius, 2002; Lin et al., 2006). As shown in this diagram, the dominant peak is <111> which are indicating that the <111> preferentially oriented XRD crystallites are formed in the film. However, the films deposited at 100ºC and 150ºC, all diffraction peaks were disappeared except weak <111> and a broad shoulder around 2θ ~27º. Results indicate the increment of crystallinity with increasing [T_{SB}] having maximum at 250ºC. It is in agreement with the Raman results as discussed before.

Figure 6 shows the variation of <111> crystallite size, [δ] and the width, [ω] of the nc-Si:H films as a function of [T_{SB}]. It can be estimated using the following equation:

$$[\delta] = \frac{k\lambda}{\beta\cos\theta} \tag{3}$$

where k, λ, β and θ are a constant, the wavelength of X-ray (1.54 Å), the full width at half maximum (FWHM) and Bragg angle of the diffraction peak respectively.

As shown in this diagram, [δ] is found to be increased with increasing [T_{SB}] having maximum value at ~6.4 nm for [T_{SB}] = 250ºC and opposite relationship is observed for [ω] as shown in Figure 6.

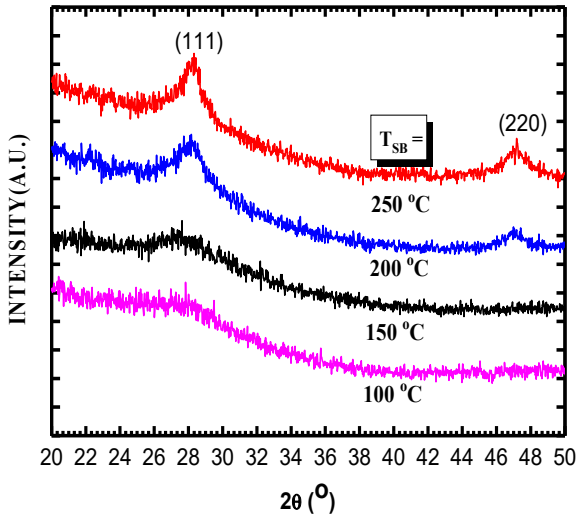

Figure 5. XRD spectra of the nc-Si:H films deposited on glass substrates at different [T_{SB}]

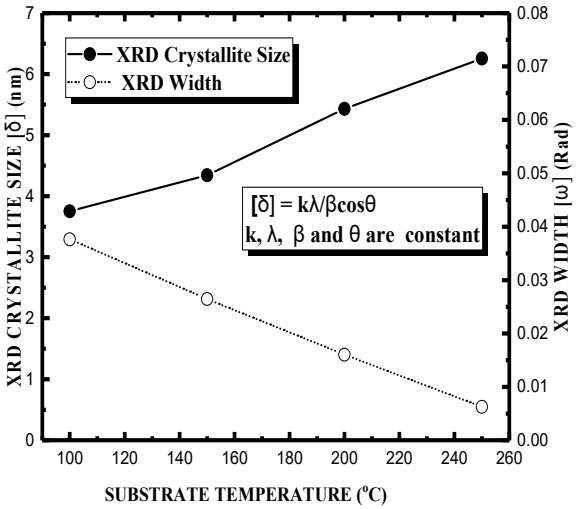

Figure 6. Dependence of XRD <111> crystallite sizes and width as a function of [T_{SB}] for the films deposited on glass substrates

3.4 Evaluation of Optical Energy (E_g) and Tauc's Slope ($B^{1/2}$) Measurements

Figure 7 shows the plots of the optical energy gap (E_g) and Tauc's slope, $B^{1/2}$ as a function of substrate temperature [T_{SB}]. The E_g and $B1^{/2}$ values of the nc-Si:H films are increasing as a function of [T_{SB}]. As shown in Figure 2, [R_D) and [n] were increasing with increasing [T_{SB}] having maximum at 250ºC due to increase in hydrogen etching effect during treatment process.

Similarly in Figure 6 shows, the average <111> grain size is the largest at 250ºC. Moreover, the high E_g and $B^{1/2}$ values as shown in Figure 7 it is clearly evident the presence of quantum confinement effects as the crystallites form a continuous structure embedded in amorphous silicon matrix structure. This result is also consistent with the results shown in Figure 3 and Figure 4. It is observed that the E_g (~ 1.9 eV) and $B^{1/2}$ [~750 $(cm.ev)^{-1/2}$] are found to be the highest where the maximum [δ] = 6.4 nm and [ρ] = 95% at [T_{SB}] = 250 ºC.

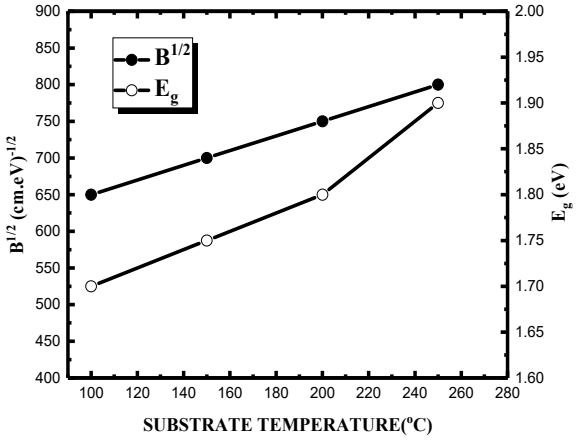

Figure 7. Variation of $B^{1/2}$ and E_g of nc-Si:H thin films as a function of substrate temperature

3.5 Bonding Properties of nc-Si:H Films Based on FT/IR Measurements

In order to understand the bonding properties of silicon with hydrogen and oxygen in the network, FTIR measurements have been studied with samples on Si-wafers. Figure 8 shows the FTIR absorbance spectra of the PECVD nc-Si:H films prepared at different substrate temperature ([T_{SB}]). In this diagram, the spectra at approximately 650 cm^{-1}, 1045 cm^{-1}, 1215 cm^{-1}, 1631 cm^{-1}, 2112 cm^{-1} and 3333 cm^{-1} are assigned to the SiH wagging, SiO stretching, SiH_2 bending, C=O, SiH_2, Si-H polyhydride Stretching and Si-OH bands respectively.

The SiH_2 band at approximately 1215 cm^{-1} is due to dihydride (SiH_2) (Wang, Lin, & Huan, 2003; Chaâbane, Cabarrocas, & Vach, 2004). The absorption at approximately 1000–1100 cm^{-1} is due to the SiO stretching band. We can compare these IR spectra, because the films have approximately the same thickness values. As shown above, the existence of Si-H_2 bending absorption bands suggest the evidence of nanocrystalline structure of these films.

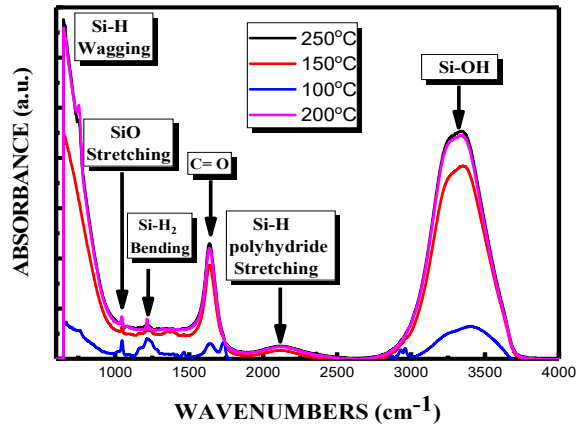

Figure 8. shows the IR absorption spectra over the range of 600–4000 cm^{-1} for nc-Si:H thin films as a function of [T_{SB}]

The bonded hydrogen (C_{SiH2}) and oxygen content (C_{SiO2}) have been estimated from Si-H_2 bending and SiO stretching bands respectively using the following equations:

$$[CSiH2 \text{ or } SiO2] = \left(\frac{A_\omega}{N_{Si}}\right)\int \alpha \frac{d\omega}{\omega} \text{ x } 100 \text{ at. \%} \quad (4)$$

where A_ω= 1.6 x10^{19} cm^{-2} and (oscillation strength) and N_{Si} = 5 x 10^{22} cm^{-3} (Density of c-Si).

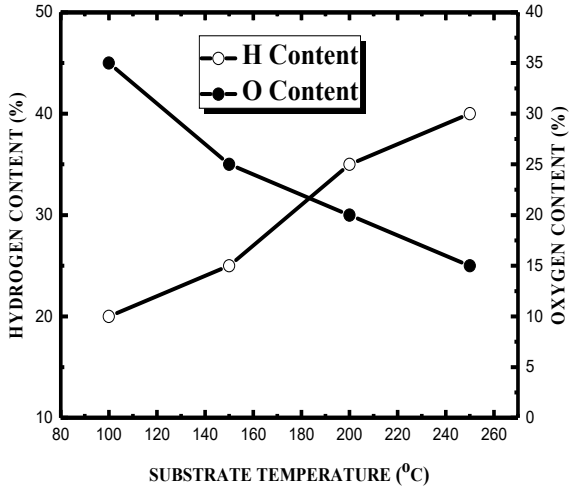

Figure 9. shows the variation of hydrogen and oxygen content as a function of [T_{SB}]

Figure 9 shows the Oxygen content decreases and Hydrogen content increases as a function of [T_{SB}]. The open and closed symbols represent C_H and C_{SiO}, respectively. As shown in this fig, the shifting of SiH_2 bending band and SiO stretching band towards the higher wave number are consistent with relatively sharp increment of hydrogen content (~20% to 40%) and sharp reduction of oxygen content (~30% to 15%) in the films as a function of [T_{SB}] corresponding to the attainment of the highest crystallinity at [T_{SB}] = 250 ºC in the network.

Table II. Summary of different component of IR spectrum obtained from transmission peak analysis of the spectrum in the range of 600cm^{-1} -3500 cm^{-1}

[T_{SB}] (ºC)	SiH Wagging (cm^{-1})	C=O (cm^{-1})	SiH Stretching (cm^{-1})	Si-OH (cm^{-1})
100	668.72	1634.9	2117.5	3319.3
150	662.45	1663.3	2117	3348.9
200	655.70	1626.2	2117.5	3311.3
250	649.92	1635.8	2117	3336.3

3.6 Evaluation of Surface Morphology Based on SEM Measurements

Scanning electron microscopy (SEM) is a branch of microscopy that produces images of a sample by scanning the surface with a focused beam of electrons. The electrons interact with atoms in the sample, producing various signals that contain information about both the sample's surface morphology, and composition (Roszairi & Rahman, 2002). The electron beam is scanned, and the beam's position is combined with the detected signal to produce images. As shown in Figure10, at 250ºC uniform grains were observed on glass substrate which is showing the highest crystallinity.

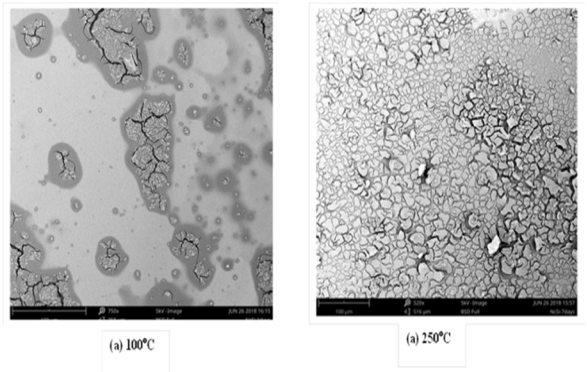

Figure 10. SEM of nc-Si:H thin films deposited at (a) 100ºC and (b) 250 ºC

3.7 Evaluation of Surface Morphology Based on AFM Measurements

Figure 11 shows AFM images for the surface of nc-Si:H films under (a) [T_{SB}] = 100 ºC, (b) [T_{SB}] = 150 ºC, (c) [T_{SB}] = 200 ºC and (d) [T_{SB}] = 250ºC. The degree of surface roughness is the root mean square (rms) value of the roughness heights. It reveals that the roughness of the nc-Si:H surfaces are found to be 68.48 nm for 100 ºC, 58.94 nm for 150 ºC, 58.34 nm for 200 ºC and 55.37 nm for 250 ºC respectively. As shown in theses diagram at [T_{SB}] = 250ºC, surface roughness is largely reduced and the roundish-like roughness having uniform heights with homogeneous grains distribution were observed (He et al., 1994; Mukhopadhyay, Chowdhury, & Ray, 2006). These results are well consistent with the results of Raman and XRD measurements.

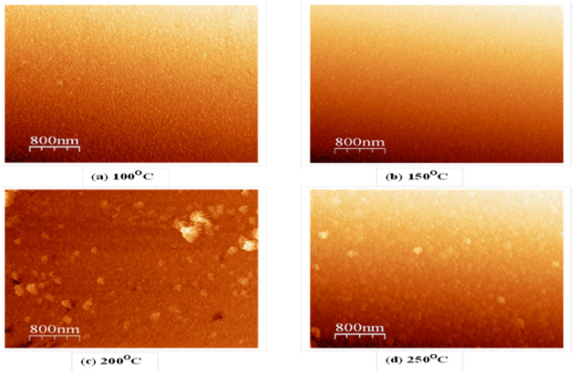

Figure 11. AFM images of the surface of nc-Si:H films deposited on glass substrates at (a) 100ºC, (b) 150ºC and (c) 200ºC and (d) 250ºC respectively

3.8 Evaluation of Electrical Properties Based on Resistivity and Hall Mobility Measurements

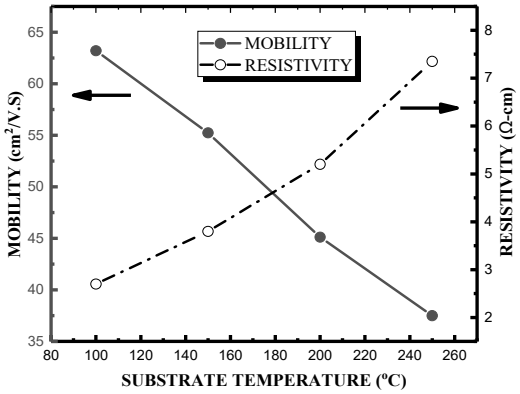

Figure 12. Mobility and Resistivity measurements of nc-Si:H films deposited on glass substrates at different [T_{SB}]

Figure 12 shows the dependence of hall mobility and the resistivity of nc-Si:H thin films as a function of [T_{SB}]. Mobility and resistivity are showing opposite relationships to each other having the minimum mobility of ~37.5 cm^2/v.s and the maximum resistivity of ~7.35 Ω-cm at 250ºC respectively (Vallat-Sauvain, Shah, & Bailat, 2006; Jana, Das, & Barua, 2002; Kamiya et al., 1999; Stieler et al., 2006; Agarwal et al., 2004; Das, 1995).

4. Discussion

In this work, the effects of substrate temperature of nc-Si:H on the structural, optical and electrical properties prepared using glow discharged decomposition technique. The deposition rate and refractive index were found to be increased with increasing substrate temperature. Crystalline volume fraction and crystalline size were showing opposite character to each other. Optical energy gap and Tauc's slope were shown ~ 1.9 eV and ~750 $(cm.ev)^{-1/2}$ respectively having maximum [δ] = 6.4 nm and [ρ] = 95% with uniform grain distributions at [T_{SB}] = 250ºC. Results indicate that *in situ* hydrogen cleaning effects is governing at the highest substrate temperature

(250ºC). At that stage high density of Si-Si bonds are localized and it forms highly ordered film structure exhibiting quantum size effects.

Acknowledgements

The authors would like to thank Dr. Sherry Painter, division chair of LeMoyne-Owen College for her support during this work. Special thanks to Dr. Delphia Harris, professor of chemistry at LeMoyne-Owen College for her helpful suggestions. We would also like to acknowledge the financial support from NSF (Grant # HRD-1332459). This work was also supported by the University Malaya Research Grant (UMRG) Program of RP007B-13AFR and University of Malaya Research Grant of RG259-13AFR.

References

Agarwal, S., Hoex, B., van de Sanden, M. C. M., Maroudas, D., & Aydil, E. S. (2004). Hydrogen in Si–Si bond center and platelet-like defect configurations in amorphous hydrogenated silicon. *Journal of Vacuum Science & Technology B: Microelectronics and Nanometer Structures Processing, Measurement, and Phenomena*, *22*(6), 2719-2726.

Chaâbane, N., i Cabarrocas, P. R., & Vach, H. (2004). Trapping of plasma produced nanocrystalline Si particles on a low temperature substrate. *Journal of non-crystalline solids*, *338*, 51-55.

Cullity, B. D. (1978). *Answers to problems: elements of X-ray diffraction*. Addison-Wesley Publishing Company.

Das, D. (1995). *Solid State Phenom, 44-46*, 227-258.

Gudovskikh, A. S., Kleider, J. P., Afanasjev, V. P., Kazak-Kazakevich, A. Z., & Sazanov, A. P. (2004). Investigation of nc-Si inclusions in multilayer a-Si: H films obtained using the layer by layer technique. *Journal of non-crystalline solids*, *338*, 135-138.

He, Y., Yin, C., Cheng, G., Wang, L., Liu, X., & Hu, G. Y. (1994). The structure and properties of nanosize crystalline silicon films. *Journal of Applied Physics*, *75*(2), 797-803.

Jana, M., Das, D., & Barua, A. K. (2002). Promotion of microcrystallization by argon in moderately hydrogen diluted silane plasma. *Solar energy materials and solar cells*, *74*(1-4), 407-413.

Kamiya, T., Nakahata, K., Miida, A., Fortmann, C. M., & Shimizu, I. (1999). Control of orientation from random to (220) or (400) in polycrystalline silicon films. *Thin Solid Films*, *337*(1-2), 18-22.

Lin, C. Y., Fang, Y. K., Chen, S. F., Lin, P. C., Lin, C. S., Chou, T. H., ... & Lin, K. I. (2006). Growth of nanocrystalline silicon thin film with layer-by-layer technique for fast photo-detecting applications. *Materials Science and Engineering: B*, *127*(2-3), 251-254.

Liu, X. N., Tong, S., Wang, L. C., Chen, G. X., & Bao, X. M. (1995). Photoluminescence of nanocrystallites embedded in hydrogenated amorphous silicon films. *Journal of applied physics*, *78*(10), 6193-6196.

Matsuda, A. (2004). Microcrystalline silicon.: Growth and device application. *Journal of Non-Crystalline Solids*, *338*, 1-12.

Mukhopadhyay, S., Chowdhury, A., & Ray, S. (2006). Substrate temperature dependence of microcrystalline silicon growth by PECVD technique. *Journal of non-crystalline solids*, *352*(9-20), 1045-1048.

Ray, S., Mukhopadhyay, S., Jana, T., & Carius, R. (2002). Transition from amorphous to microcrystalline Si: H: effects of substrate temperature and hydrogen dilution. *Journal of non-crystalline solids*, *299*, 761-766.

Ritikos, R., Goh, B. T., Sharif, K. A. M., Muhamad, M. R., & Rahman, S. A. (2009). Highly reflective nc-Si: H/a-CNx: H multilayer films prepared by rf PECVD technique. *Thin Solid Films*, *517*(17), 5092-5095.

Roszairi, H., & Rahman, S. A. (2002, December). High deposition rate thin film hydrogenated amorphous silicon prepared by dc plasma enhanced chemical vapour deposition of helium diluted silane. In *Semiconductor Electronics, 2002. Proceedings. ICSE 2002. IEEE International Conference on* (pp. 300-303). IEEE.

Roszairi, H., & Rahman, S. A. (2002, December). High deposition rate thin film hydrogenated amorphous silicon prepared by dc plasma enhanced chemical vapour deposition of helium diluted silane. In *Semiconductor Electronics, 2002. Proceedings. ICSE 2002. IEEE International Conference on* (pp. 300-303). IEEE.

Stieler, D., Dalal, V. L., Muthukrishnan, K., Noack, M., & Schares, E. (2006). Electron mobility in nanocrystalline silicon devices. *J.Appl.Phys., 100*, 036106.

Tsu, R., Gonzalez-Hernandez, J., Chao, S. S., Lee, S. C., & Tanaka, K. (1982). Critical volume fraction of crystallinity for conductivity percolation in phosphorus-doped Si: F: H alloys. *Applied Physics Letters*, *40*(6), 534-535.

Vallat-Sauvain, E., Shah, A., & Bailat, J. (2006). Advances in microcrystalline silicon solar cell technologies. *Thin Film Solar Cells: Fabrication, Characterization, and Application*, *1*, 133-171.

Wang, Y. H., Lin, J., & Huan, C. H. A. (2003). Structural and optical properties of a-Si: H/nc-Si: H thin films grown from Ar–H2–SiH4 mixture by plasma-enhanced chemical vapor deposition. *Materials Science and Engineering: B*, *104*(1-2), 80-87.